



## Research Note

# Optimum Orientation of the Multi-Span Greenhouse for Maximum Capture of Solar Energy in Central Region of Iran

Mehran Gheyrati, Asadollah Akram, Hassan Ghasemi-Mobtaker\*

Department of Agricultural Machinery Engineering, Faculty of Agricultural Engineering and Technology, University of Tehran, Karaj, Alborz, Iran.

### PAPER INFO

#### Paper history:

Received: 22 September 2021  
Revised in revised form: 16 February 2022  
Scientific Accepted: 16 February 2022  
Published: 02 July 2022

#### Keywords:

Greenhouse Orientation,  
Mathematical Modeling,  
North Wall,  
Solar Irradiation

### ABSTRACT

The orientation of greenhouses is one of the effective factors in terms of radiation they receive. In the present study, a multi-span greenhouse (40 m × 93.5 m with a coverage area of 5457.44 m<sup>2</sup>) located in the central region of Iran was investigated in three orientations including: North-South (N-S), East-West (E-W), and Northeast-Southwest (NE-SW: the most frequent orientation of the existing greenhouses in the study area). The solar irradiation received on the outside surface of the greenhouse cover and the amount of irradiation captured inside the greenhouse for each orientation during the cold season were calculated using mathematical modeling and the results were compared. According to the results, in the E-W orientation, the main sections of receiving solar irradiation, such as the south and north roofs, have a better angle toward the sun; therefore, the quantity of solar irradiation captured inside the greenhouse with the E-W orientation was on average 361.48 MJ day<sup>-1</sup> more than that with the N-S orientation. The north wall of the greenhouse could not receive the beam radiation for all the orientations investigated, and the total irradiation captured by this section was composed of the diffused radiation and the ground-reflected radiation, which is an important result for insulation of some surfaces of greenhouses.

<https://doi.org/10.30501/jree.2022.305780.1259>

## 1. INTRODUCTION

Achieving food security and reducing environmental pressures require convergence towards healthy and adequate diets. Such a convergence would require increasing the quantity and quality of food supply for many areas [1]. However, 30 % of the world's food is lost due to transportation because of the distance of food production centers from consumers. Controlled Environment Agriculture (CEA), including greenhouse crop production, enables the production of crops outside the climate and their seasons. Prolonging of seasonal crops cultivation periods allows for agricultural crops to be produced beside consumption locations which, in turn, decrease transportation distances [2]. Greenhouse cultivation is one of the main and popular methods to meet the growing need for food universal because compared with field cultivation, it has a so great production [3]. Greenhouse is a structure that provides a suitable environment for plants' production, especially in cold weather.

Due to Iran's locations in arid and semi-arid climates, the development of greenhouses is one of the main programs of the agricultural sector. In recent years, the development of greenhouses in Iran has been seriously pursued and the covered area by the greenhouses has increased from 8,000 ha

to 18,500 ha [4]. Yazd province with more than 1970 greenhouse holdings is one of the most important centers for greenhouse crop production in Iran [5].

The high output requires investment cost, labor, fertilizers, and energy input [6]. The high cost of input energy in greenhouse cultivation is one of the main issues. For greenhouse cultivation in cold weather, the main operating cost after labor is related to energy cost. The major portion of the total energy used in greenhouses (65-85 %) is consumed for heating, and the remainder is used for transportation and electrical equipment [7].

In addition to increasing operating costs, energy supply through fossil fuels also raises environmental issues. About 14 % of the world's net CO<sub>2</sub> emissions come from the agriculture sector [8]. For sustainable energy consumption management, three significant aspects should be considered: energy use, environmental effects, and economic efficiency [9]. Hence, there is a need to use clean energy to reduce environmental impact and operating costs. Solar radiation, as a renewable energy origin, is one of the main sources of clean energy in Iran. In Yazd province, the solar irradiation on the horizontal surface is about 7787 MJ/m<sup>2</sup> yr [10]. This great amount of solar irradiation can be applied to greenhouse heating and reduction of fossil fuel consumption.

There are some studies carried out on enhancing the greenhouse heating systems and improve use of solar energy

\*Corresponding Author's Email: [mobtaker@ut.ac.ir](mailto:mobtaker@ut.ac.ir) (H. Ghasemi-Mobtaker)  
URL: [https://www.jree.ir/article\\_152883.html](https://www.jree.ir/article_152883.html)



inside the greenhouse [11-20]. Yildirim and Bilir [21] modeled a greenhouse in Izmir, Turkey to survey the feasibility of using renewable energy to meet greenhouse energy needs. The greenhouse with an area of 150 m<sup>2</sup> and three different crops (lettuce, tomato, and cucumber) was investigated. According to the results, with a 21510.4 kWh total electrical energy production of solar cell system, annual coverage ratio values for energy demand of lettuce, tomato, and cucumber are estimated as 104.5 %, 95.7 %, and 86.8 %, respectively. Wei et al. [22] studied two greenhouses types with mobile behind walls to enhance the thermal efficiency of popular single-span greenhouses in China. The mobile behind walls were built of jute fiber boards and were fixed in winter for heat maintenance. The results demonstrated that two types of greenhouses with mobile behind walls could be a better alternative to the popular greenhouse. Also, studies on design principles including the shape and optimal orientation of greenhouses have been conducted for receiving maximum solar radiation. Von Elsner et al. [23] examined the structural requirements of greenhouses in Europe. They reported that compared with N-S orientation, in E-W orientation toward solar radiation passing through greenhouse cover is more in winter and lower in summer. The transmission of solar radiation depends on the sun elevation. Kendirli [24] analyzed greenhouse structures in Turkey. Among the greenhouses studied, 85 % were situated in the E-W orientation and 15 % in the N-S orientation. According to the results, because most of the small family enterprises in the area have single rows, construction of greenhouses in E-W orientation enhances the efficiency of solar energy.

Sethi [25] investigated five popular single-span greenhouses to determine the most appropriate greenhouse shape and orientation. To this end, a mathematical model was developed for computing total transmitted solar radiation through walls, roofs, and inclined surfaces. Greenhouses were investigated for both E-W and N-S orientations. The results showed that uneven-span greenhouse captured the maximum solar energy. In addition, the E-W orientation was the best direction of the greenhouse, because this orientation receives less energy in summer and more energy in winter (except for regions near the equator). Also, for the same greenhouse shape, the amount and pattern of solar radiation availability vary at different latitudes. In another study, the five popular greenhouses were investigated with the aim of optimizing energy consumption in the colder months of the year for a composite climate. To this end, the steady state analysis was developed and numerical calculations were performed for the Delhi climate of India. The greenhouses were single-span shapes and studied in an E-W orientation. According to the results, in the composite climate, the uneven span greenhouse is the best selection and LPG remains the most appropriate fuel for providing additional fuel needs for the given condition [26].

Çakır and Şahin [27] investigated the feasibility of greenhouses use in cold regions. They studied five different shapes of single-span greenhouses and developed a model in MATLAB software for estimating the availability of solar energy. Evaluation comparison was conducted for a greenhouse located in Bayburt, northeastern Anatolia, Turkey. The results indicated that the optimum shape of greenhouse for Bayburt conditions was elliptic. Type shape and of the roof was also the most important parameter affecting the amount of solar radiation received by greenhouses. The greenhouse roof shape and orientation play an important role in using the maximum possible received energy. In another

study in the north tropical region (latitude: 24° to 31.2°) for the single-span greenhouse, the value of solar energy that can be captured by the greenhouse was calculated. According to the results, the ellipse aspect ratio has a great effect on the received solar radiation. In addition, the greenhouse orientation was recommended with respect to south direction because this orientation captured the maximum heat value [28].

The heat demand of the greenhouse depends on its location and shape. Therefore, a local survey is of major significance to modeling the greenhouse loads and supplying portion of the needed energy from renewable energy sources. Accordingly, a study was conducted in Romania (latitude 44.25°N) with the aim of making a comparison between two different orientations of an even-span shape greenhouse. Based on the simulation results, the E-W orientation was advantageous all year along from the energy loads standpoint [29].

In the regions located in the northern hemisphere, the orientation of solar greenhouses has a great effect on the amount of captured solar radiation. Thus, applying Extreme Value Theory, Chen et al. [30] proposed a method to assess the best orientation for Chinese solar greenhouses considering the impact of geographical latitude. They reported that the best orientation depended on the solar greenhouse latitude and for northern China, the solar greenhouse orientation must be from South to West. Ghasemi-Mobtaker et al. [31] compared the solar radiation availability for six different shapes of single-span greenhouses in Tabriz, Iran (latitude 38°N). A dynamic model was used to model all the greenhouse internal temperatures. According to the modeling results, the E-W orientated single-span greenhouse captured the highest amount of solar radiation in winter. In addition, using a northern brick wall can greatly reduce entered radiation loss. Chen et al. [32] established a mathematical model to choose the optimal shape and orientation of the greenhouse in cold season with the aim of receiving the maximum solar energy. The results demonstrated that the greenhouse orientation had a significant effect on the total solar irradiation captured by the greenhouse and that the E-W orientation in southern China was an optimal selection. The latitude also had a significant effect on the greenhouse solar radiation availability, such that upon the increasing latitude, the global solar radiation received in greenhouse decreased gradually in cold season.

Research in different parts of the world indicates that it is not possible to comprehensively make a single recommendation for all latitudes. Thus, for important and developing areas of greenhouse cultivation, the optimal orientation of structures with respect to latitude, climate, and environmental factors specific to the same area should be studied in order to ensure a safe and sustainable investment. Most of the reviewed studies targeted single-span greenhouses, while commercial greenhouses are multi-span and large-scale. Therefore, the findings on solar radiation captured in this group of greenhouses can be important to the agricultural operators. In addition, the study of radiation received for each surface of the structure and the type of radiation is important for researchers and is, also, useful to continue research on the study of energy saving techniques.

In this study, mathematical modeling for the multi-span greenhouse was performed with the aim of determining the optimum orientation in terms of the maximum solar energy captured. Hourly irradiation received on the outer surface of the cover and the irradiation captured inside were calculated for each surface of the structure using total solar radiation

measured on the horizontal surface. For a more detailed study and considering the environmental conditions of the study area, the received solar irradiation was calculated for the dominant orientation of the greenhouses in this region and the results was compared with the two main orientations (E-W and N-S). Moreover, this study investigated the effect of north wall insulation on the amount of energy received inside greenhouses.

## 2. MATERIALS AND METHODS

### 2.1. Region of study

This study was conducted in the Hemmatabad region, Yazd province, located at the center of Iran, at a geographical location of 54°8' east longitude and 32°2' north latitude. Hemmatabad region with an area of 75 ha under greenhouse cultivation and an average annual production of 22,500 ton of greenhouse crops is one of the most important areas for the collection of greenhouse units in Yazd province [4]. The experimental site with hyper arid-cold (according to De Martonne climate classification) is 1140 m above the sea level [33]. As shown in Figure 1, the northeast-southwest direction is the dominant orientation of the greenhouses in the Hemmatabad region.

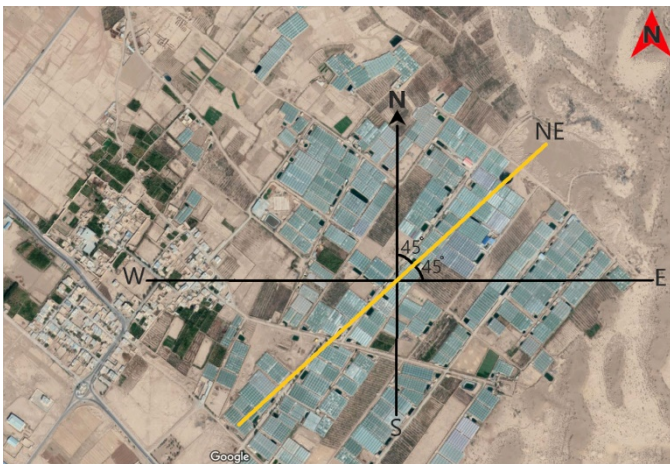


Figure 1. Aerial view of greenhouses in Hemmatabad district

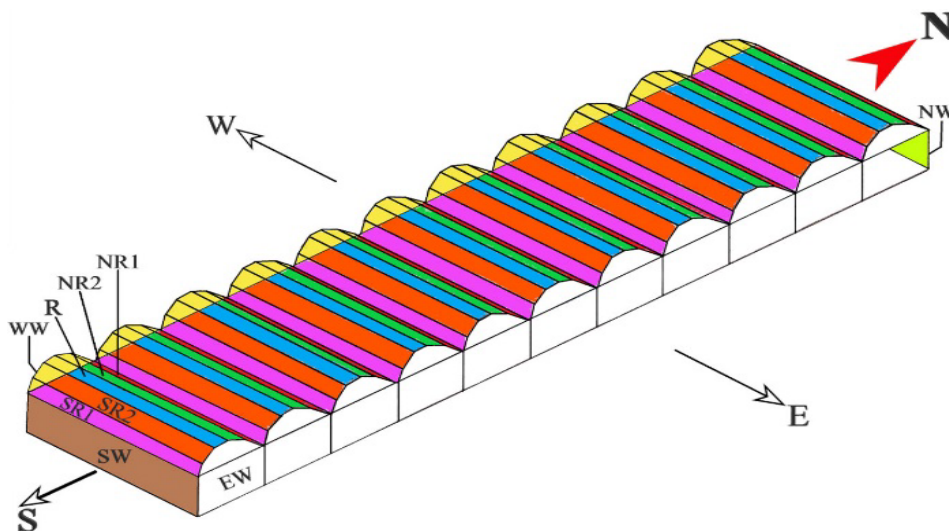
### 2.2. Greenhouse model

In this study, the effect of orientation on solar irradiation received inside the greenhouses is investigated. For this purpose, a greenhouse with the specifications given in Table 1 was considered in three directions: north-south (N-S), east-west (E-W), and northeast-southwest (NE-SW). In addition, the received radiation was calculated for each orientation and the results were compared with each other. Due to the type and dimensions of most of the existing structures built in the last few years in the study region, a greenhouse with the assumptions of Table 1 was modeled in this study. Considering the latitude of the study region, arch height, and its ratio to the center height ( $\frac{2}{7}$ ) and due to the lack of effective shading of the roofs on each other, it is assumed that the shadow of the roof does not occur.

For computation purposes, the small curved section surfaces (canopy) have been considered as flat surfaces [25]. The conversion of all surfaces of the greenhouse curve into flat plates, along with their naming for one span, is shown in Figure 2 for E-W orientation greenhouse. Moreover, the specifications of each section are given in Table 2. For each of the surfaces introduced in Figure 2, the surface slope angle ( $\beta$ : the angle between the plane of the surface in question and the horizontal) and surface azimuth angle ( $\gamma$ : the deviation of the projection on the horizontal plane of the normal to the surface from the local meridian) for the studied greenhouses are shown in Table 2.

Table 1. Model greenhouse specifications

Parameter	Value
Geometry	Arch / Multi-span
Length	40 m
Arch span	8.5 m
Number of spans	11
Total width	93.5 m
Area	3740 m <sup>2</sup>
Column height	4 m
Arch height	1.6 m
Center height	5.6 m
Cover	polyethylene
Total coverage area	5457.44 m <sup>2</sup>



SW: south wall, SR: south roof, R: horizontal roof, NW: north wall, NR: north roof, EW: east wall, WW: west wall

Figure 2. Conversion of curved surfaces into flat plates and assigning them for one span of the greenhouse (E-W)

**Table 2.** Sectional specifications of one span of the greenhouse in the investigated orientations

Sectional specifications in the E-W orientation									
	SW	SR 1	SR 2	R	NW	NR 1	NR 2	EW	WW
Area (m <sup>2</sup> )	160	76	76	76	160	76	76	43.52	43.52
$\beta$ (°)	90	33	16	0	90	33	16	90	90
$\gamma$ (°)	0	0	0	—	180	180	180	-90	90
Sectional specifications in the N-S orientation									
	EW	ER 1	ER 2	R	WW	WR 1	WR 2	NW	SW
Area (m <sup>2</sup> )	160	76	76	76	160	76	76	43.52	43.52
$\beta$ (°)	90	33	16	0	90	33	16	90	90
$\gamma$ (°)	-90	-90	-90	—	90	90	90	180	0
Sectional specifications in the NE-SW orientation									
	SE.W*	SE.R 1	SE.R 2	R	NW.W	NW.R 1	NW.R 2	NE.W	SW.W
Area (m <sup>2</sup> )	160	76	76	76	160	76	76	43.52	43.52
$\beta$ (°)	90	33	16	0	90	33	16	90	90
$\gamma$ (°)	-45	-45	-45	—	135	135	135	-135	45
* SE.W: Southeast wall, SE.R: Southeast roof, R: Horizontal roof, NW.W: Northwest wall, NW.R: Northwest roof, NE.W: Northeast wall, SW.W: Southwest wall									

### 2.3. Beam and diffuse components of hourly irradiation

The hourly solar irradiation received on the horizontal surface on a day of three colder months of the year (December, January, and February) from 2009 to 2019 was gathered from

$$\frac{I_d}{I} = \begin{cases} 1.0 - 0.09k_t & k_t \leq 0.22 \\ 0.9511 - 0.1604k_t + 4.388k_t^2 - 16.638k_t^3 + 12.366k_t^4 & 0.22 < k_t \leq 0.80 \\ 0.165 & k_t > 0.80 \end{cases} \quad (1)$$

The hourly clearness index ( $k_t$ ) is the ratio of particular hourly irradiation received on the horizontal surface to the extraterrestrial irradiation for that hour [35].

### 2.4. Solar radiation on inclined surfaces

The total radiation received on greenhouse roofs and walls was considered to be having 3 components: beam radiation, diffuse radiation, and radiation reflected from the ground. Based on this concept and by applying Eq. (2), the total solar irradiation on any surfaces of greenhouse per square meter were calculated [36]:

$$S_i(t) = I_b R_{b,ave} + I_d R_d + (I_b + I_d) \rho R_r \quad (2)$$

Each of the components of this expression is as follows:

#### 2.4.1. Beam radiation availability on greenhouse cover

The relation between the beam radiation on the horizontal surface and that on the tilted surface ( $R_b$ ) can be computed as follows [26, 35]:

$$R_b = \frac{\cos \theta_i}{\cos \theta_z} \quad (3)$$

To extend Eq. (3) to an integrated form from an instantaneous equation (limits  $\omega_1$  and  $\omega_2$  defined in an hour) over a time period of  $\omega_1$  to  $\omega_2$ , the average  $R_b$  is given by [35]:

the Islamic Republic of Iran Meteorological Office data center (IRIMO) in Yazd province.

To calculate the irradiation receiving the inclined surfaces, the contributions of diffuse and beam irradiation of global radiation on the horizontal surface must first be determined, for which purpose Eq. (1) was used [34, 35]:

$$R_{b,ave} = \frac{\int_{\omega_1}^{\omega_2} \cos \theta_i d\omega}{\int_{\omega_1}^{\omega_2} \cos \theta_z d\omega} \quad (4)$$

where

$$\int_{\omega_1}^{\omega_2} \cos \theta_i d\omega = (\sin \delta \sin \Phi \cos \beta - \sin \delta \cos \Phi \sin \beta \cos \gamma) \frac{1}{180} (\omega_2 - \omega_1) \pi + (\cos \delta \cos \Phi \cos \beta + \cos \delta \sin \Phi \sin \beta \cos \gamma) (\sin \omega_2 - \sin \omega_1) - (\cos \delta \sin \beta \sin \gamma) (\cos \omega_2 - \cos \omega_1) \quad (5)$$

and:

$$\int_{\omega_1}^{\omega_2} \cos \theta_z d\omega = (\cos \Phi \cos \delta) (\sin \omega_2 - \sin \omega_1) + (\sin \Phi \sin \delta) \frac{1}{180} (\omega_2 - \omega_1) \pi \quad (6)$$

#### 2.4.2. Diffuse radiation and radiation reflected from the earth's ground

Some parts of the solar radiation reach the earth's surface after scattering in the atmosphere. The current study assumes that

the solar diffuse radiation in the atmosphere is isotropic (the diffuse radiation from the whole sky is of the same strength approximately). Thus, to determine the diffuse radiation received by a face tilted from the horizontal at slope  $\beta$ , first, the view factor of surface to the sky was calculated [26, 35]:

$$R_d = \frac{1 + \cos \beta}{2} \quad (7)$$

To calculate the solar radiation diffusely reflected from the earth's surface and received by a surface with a slope  $\beta$  relative to the horizontal, the view factor for the earth's surface was calculated:

$$R_r = \frac{1 - \cos \beta}{2} \quad (8)$$

Each type of ground reflects radiation differently; thus, the ground reflection factor ( $\rho$ ) is used.  $\rho$  is the so-called albedo value (ALB) and its value for heath surfaces is 0.10 to 0.25 [37]. In the present case, in terms of the land type and vegetation of the investigated region, the value of 0.25 has been applied.

## 2.5. Solar radiation received on greenhouse cover

Total solar radiation falling on the outer surface of greenhouse cover is thus calculated as follows [31]:

$$S_t = \sum S_i(t)A_i \quad (9)$$

In the case of the multi-span greenhouse under investigation, there are several roofs and walls whose factors mentioned in Table 2 (depending on the orientation) are the same for some of their surfaces. Therefore, calculations are performed for one of these surfaces and the result is multiplied by their number. As shown in Figure 2, the flat plates that receive equal radiation are shown in the same color.

## 2.6. Solar radiation transmission from greenhouse cover

The entire radiation on the outer surface of the greenhouse cover does not reach the environment; instead, some of it is reflected by the greenhouse cover, some is absorbed by the cover while the remainder is transferred to the inside environment of the greenhouse. The initially transmitted solar radiation (regardless of the absorption factor of cover) dependent on parallel component ( $r_{||}$ ) and perpendicular component ( $r_{\perp}$ ) [19] is given below:

$$\tau_r = \frac{1}{2} \left[ \frac{1 - r_{||}}{1 + r_{||}} + \frac{1 - r_{\perp}}{1 + r_{\perp}} \right] \quad (10)$$

where:

$$r_{||} = \frac{\tan^2(\theta_r - \theta_i)}{\tan^2(\theta_r + \theta_i)} \quad (11)$$

$$r_{\perp} = \frac{\sin^2(\theta_r - \theta_i)}{\sin^2(\theta_r + \theta_i)} \quad (12)$$

$\theta_i$  is the incidence angle of the unpolarized radiation and considered equal to the average value at the one-hour interval.  $\theta_r$  is the refraction angle. These angles are dependent on the refraction indices in the cover medium as follows:

$$\frac{n_i}{n_r} = \frac{\sin \theta_r}{\sin \theta_i} \quad (13)$$

The values of refractive indices of air ( $n_i$ ) and polyethylene ( $n_r$ ) are taken as 1 and 1.37, respectively [25]. The absorption of solar radiation in a semi-transparent medium can be calculated based on Bouguer's law. For this reason, the following function was used [35]:

$$\tau_a = \frac{I_{\text{transmitted}}}{I_{\text{incident}}} = \exp\left(-\frac{KL}{\cos \theta_r}\right) \quad (14)$$

where  $K$  is the extinction coefficient (assumed to be a fixed in the solar spectrum) and its value was considered to be  $400 \text{ m}^{-1}$  for the polyethylene sheet [38]. The cover thickness ( $L$ ) of 0.2 mm was used for polyethylene case [25]. Finally, the transmittance coefficient of a single cover is calculated as follows:

$$\tau = \tau_r \tau_a \quad (15)$$

Equations (10)-(15) can be applied only to the solar beam radiation because its incidence angle ( $\theta_i$ ) is calculated. However, for diffuse and reflected radiation, this angle is unknown. The results presentation can be facilitated by determining an equivalent angle for solar beam radiation. Thus, for incident isotropic radiation, it is assumed that a cover has equal transmittance for reflected and diffuse radiation as it does for beam radiation event at an angle of  $60^\circ$  [35].

## 3. RESULTS AND DISCUSSION

Based on the meteorological data (from 2009 to 2019), the average of solar energy on the average day of each month was calculated for Yazd province. The average daily irradiation of solar energy for this province was about  $25 \text{ MJ m}^{-2}$ .

### 3.1. The portion of beam and diffuse irradiation

The portion of beam and diffuse components of hourly irradiation for the mean of the average days of the investigated months is illustrated in Figure 3. At Hour 12 (noon, local meridian), the maximum beam radiation occurs due to the position of the sun perpendicular to the earth and traversing of the shortest distance in the atmosphere by the sun's rays.

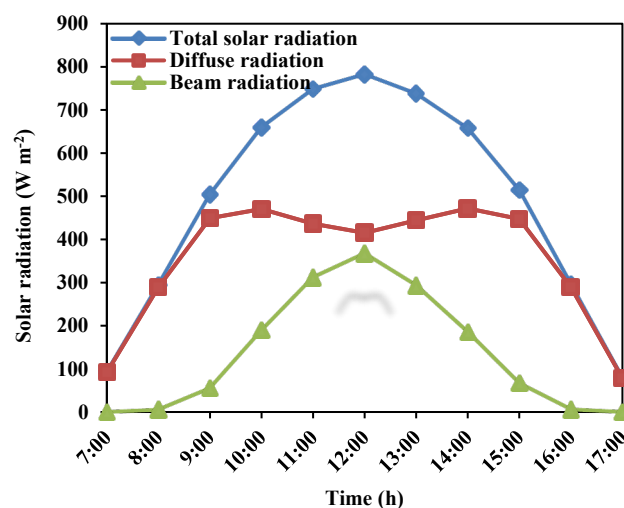


Figure 3. Share of beam and diffuse radiation of global solar radiation

### 3.2. Irradiation received on the outer surface of the cover

The most important factors in the solar irradiation captured by the greenhouse are the position of the plates relative to the sun and their view factor to the sky. The average of solar irradiation captured by the greenhouse for each orientation is illustrated in Figure 4.

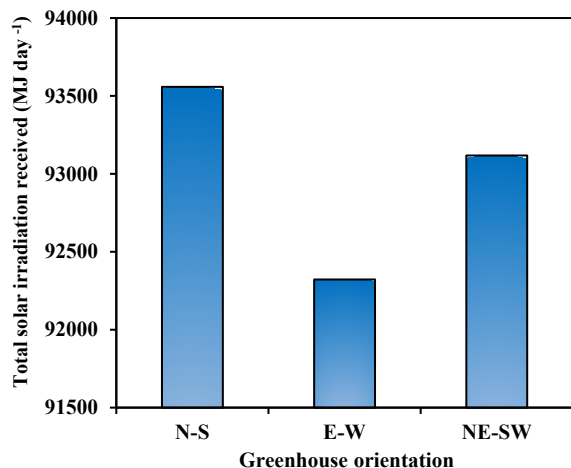


Figure 4. Total solar irradiation captured by the greenhouse for each orientation

The N-S orientation received more irradiation on the outer surface of the cover, compared to other two orientations. However, not all of this irradiation is incorporated into the inside environment of the greenhouse and the changes occur as a result of the cover transmittance.

### 3.3. Total irradiation captured inside the greenhouse

In this study, hourly transmissivity ( $\tau$ ) for each greenhouse surface on the average day (for each month) was computed. Table 3 shows this coefficient for surfaces of the greenhouse in E-W orientation on the average day of January.

According to Table 3, the West Wall (WW) in the morning and the East Wall (EW) in the afternoon did not receive beam radiation due to the sun location. Figure 5 shows the total solar radiation that the greenhouse received in each orientation.

The greenhouse captured the maximum solar irradiation in E-W orientation. Kendirli [24] reported that the east-west orientation for greenhouses in Turkey increased the solar energy efficiency. According to Table 4, the greenhouse located in the E-W orientation on 10 December captured 424.8 MJ more radiation than N-S orientation. The energy value of the natural gas is 49.5 MJ m<sup>-3</sup> [39]. Thus, in December, the E-W orientation captured more energy equivalent to 257.4 m<sup>3</sup> of natural gas than the N-S orientation.

Table 3. Transmittance coefficient for surfaces of east-west greenhouse on 17 January

Time \ Section	Beam radiation											Diffuse radiation and ground-reflected
	7:00	8:00	9:00	10:00	11:00	12:00	13:00	14:00	15:00	16:00	17:00	
SW	0.33	0.40	0.45	0.48	0.50	0.50	0.48	0.45	0.40	0.33	0.00	0.80
SR1	0.25	0.38	0.47	0.53	0.56	0.56	0.53	0.47	0.38	0.25	0.00	0.80
SR2	0.17	0.30	0.40	0.46	0.49	0.49	0.46	0.40	0.30	0.17	0.00	0.80
R	0.08	0.20	0.30	0.36	0.39	0.39	0.36	0.30	0.20	0.08	0.00	0.80
NW	0.00	0.00	0.00	0.00	0.00	0.00	0.00	0.00	0.00	0.00	0.00	0.80
NR1	0.00	0.00	0.00	0.03	0.05	0.05	0.03	0.00	0.00	0.00	0.00	0.80
NR2	0.00	0.08	0.16	0.22	0.24	0.24	0.22	0.16	0.08	0.00	0.00	0.80
EW	0.53	0.47	0.38	0.25	0.09	0.00	0.00	0.00	0.00	0.00	0.00	0.80
WW	0.00	0.00	0.00	0.00	0.00	0.09	0.25	0.38	0.47	0.53	0.55	0.80

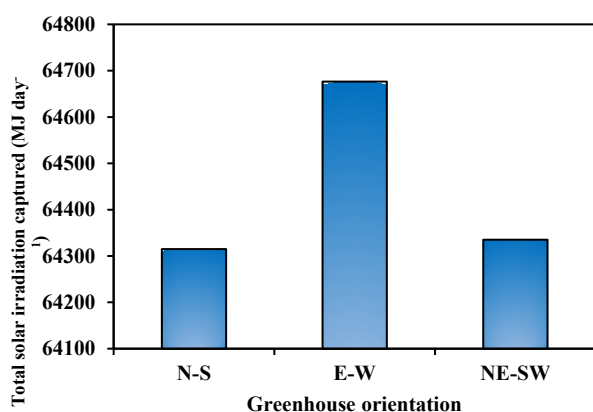


Figure 5. Total solar irradiation captured inside the greenhouse for each orientation

Table 4. Total irradiation captured in the greenhouse on average days in each orientation (MJ)

	N-S	E-W	NE-SW
10 December	59941.2	60366.0	60032.5
17 January	64985.4	65517.2	65063.0
16 February	68018.3	68146.2	67910.0
Mean of the average days	64315.0	64676.5	64335.2

Sethi [25] and Chen et al. [32] reported that the E-W orientation captured maximum solar irradiation in winter. In another study conducted at 44°N latitude, for the E-W orientation, energy saving was reported at about 125 kWh day<sup>-1</sup> in June and 87 kWh day<sup>-1</sup> in January [29].

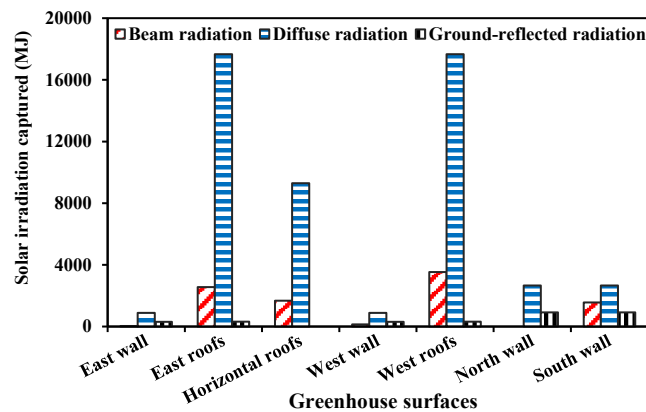
### 3.3.1. The types of irradiation received inside the greenhouse

Each type of irradiation captured inside the greenhouse is shown for each orientation and surface of the structure in Figure 6.

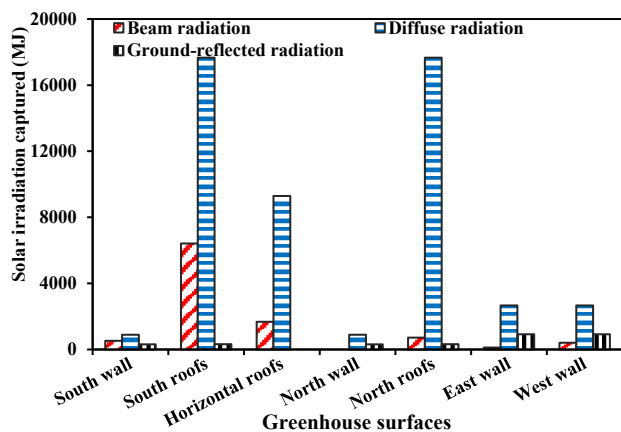
The west and east roofs in the N-S orientation captured greater irradiation than other parts of the greenhouse due to their good position relative to the sun during the day and the large area of these surfaces (1672 m<sup>2</sup> for each group of roofs in the total of structure). In Argentina, for an even span greenhouse with N-S orientation, the east roof received the highest solar irradiation in winter [13].

Figure 6 (b) shows that in the E-W orientation, the north roofs (red and green surfaces in Figure 2) and south roofs (purple and orange surfaces in Figure 2) received greater irradiation. This was due to the large area of these surfaces and their wide view factor to the sky. The horizontal roofs also received a lot of diffuse irradiation due to their maximum view factor to the sky ( $R_d=1$ ). The beam radiation was not captured by north wall of the greenhouse. Table 3 shows that the transmissivity coefficient ( $\tau$ ) of beam radiation from the north wall (for E-W orientation) was zero during the day and the total irradiation received by this section consisted of diffuse and reflected irradiation. In the NE-SW orientation, the phenomenon of non-capturing of beam radiation by the north wall occurred for both northeast and northwest walls.

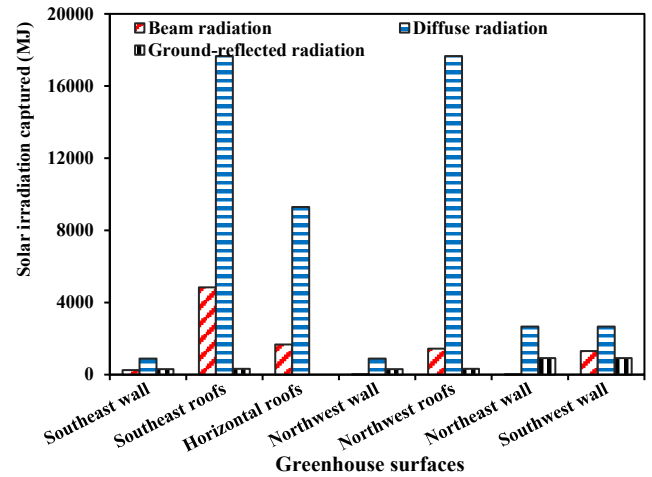
The reason for the high amount of diffuse radiation, as shown in Figure 6, is that the study was conducted for the cold season. According to Figure 3, in this season, the diffuse irradiation received on the ground's surface was much more than beam radiation.



(a)



(b)



(c)

**Figure 6.** Components of total irradiation received inside the three orientations (a: N-S; b: E-W; c: NE-SW) for each surface of the greenhouse

### 3.4. Hourly analysis of irradiation captured for each surface

The hourly variations of irradiation captured by each section (walls and roofs) of the greenhouse for N-S orientation are shown in Figure 7.

As can be seen from Figure 7, according to the direction of the east and west roofs and the path of the sun, the irradiation captured by the eastern roofs is reduced during the day and added to the irradiation received by the western roofs. Thus, it can be concluded that the sun is inclined toward these surfaces during the day. Due to this angle of inclination (solar incidence angle), not all of the irradiation received on the outer surface of the cover is added to the greenhouse and the large amount of it is wasted. Therefore, the greenhouse with N-S orientation in the cold season, despite having greater irradiation received (on the outer surface of the cover) than the E-W orientation, captured less irradiation inside the greenhouse.

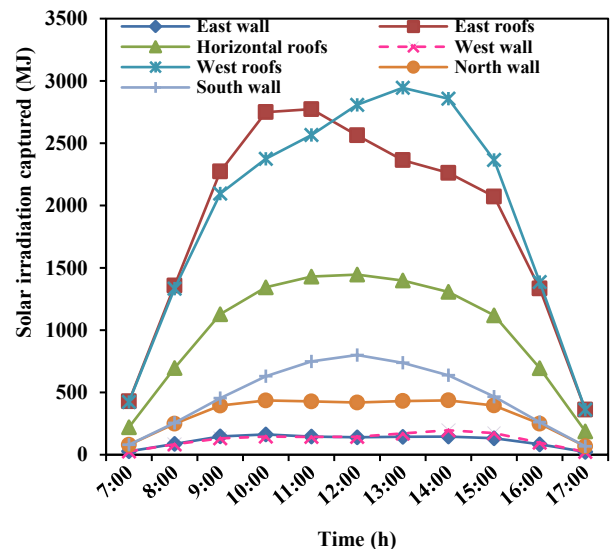


**Figure 7.** Hourly variations of irradiation received on each section of the greenhouse for the N-S orientation

Figure 8 shows that in the E-W orientation, the movement of the sun from east to west had a significant effect on the

irradiation captured by the southern roofs, and this section of the greenhouse received irradiation on a horizontal surface. Therefore, the large amount of irradiation received on the outer surface of the southern roofs was transferred from the cover and captured inside the greenhouse. In other words, the main section of the irradiation receiver in the greenhouse with E-W orientation was perpendicular to the sun; thus, greater irradiation spread into the environment, compared to the N-S orientation. Finally, it can be concluded that the solar transmittance of cover was affected by incidence angle and sun elevation. Von Elsner et al. [23] reported that for greenhouses in European Union countries, the transmittance through multi-span pitched-roof structures was lower in winter for the N-S than that for the E-W orientation.

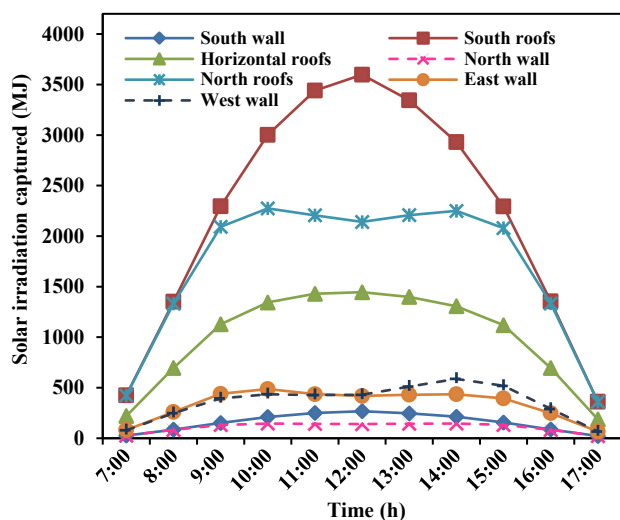


**Figure 8.** Hourly variations of irradiation captured by each surface of the greenhouse for the E-W orientation

Figure 9 shows that in the NE-SW orientation, the southeast and northwest roofs received greater irradiation. In general, it can be said that the greenhouse conditions with this orientation were in the middle of the E-W and N-S orientation. Therefore, in order to correctly understand the pattern and amount of radiation received for a greenhouse with the NE-SW orientation, calculations should be done for the whole year to evaluate its suitability than other two orientations.

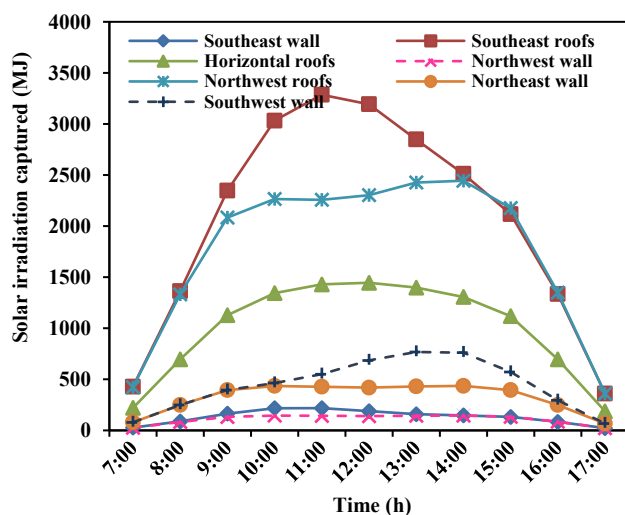


**Figure 9.** Hourly variations of irradiation captured by each surface of the greenhouse for the NE-SW orientation

In the NE-SW orientation, if the northeast wall was insulated despite the large area of this wall ( $478.72 \text{ m}^2$ ), only 5.6 % of the total irradiation captured during the day would be reduced. Ignoring this amount of captured irradiation can be justified in comparison with energy savings caused by the insulation of this surface of the greenhouse. In general, due to the non-capturing of the beam irradiation by the north wall for the three orientations, its insulation can be effective in saving energy consumption. Gupta and Chandra [12] reported that insulation of north wall in E-W oriented greenhouse could reduce 30 % of the structure's heating requirements. Also, another study demonstrated that the use of brick wall on the northern side of greenhouse with E-W orientation could reduce 31.7 % of heating demand in winter [19].

### 3.5. Importance of time of receiving maximum irradiation

According to Figure 8, the maximum solar irradiation received inside the E-W oriented greenhouse was at noon. Although this amount of energy is greater than what the greenhouse needs at noon, a large portion of it must be removed from the greenhouse by ventilation system [19]. Therefore, use of energy storage methods can be useful. Berroug et al. [40] reported that on winter nights, the application of phase change material placed in the north wall of the E-W oriented greenhouse could increase the temperature of plants and the air inside by 6–12 °C. On the other hand, Figure 7 shows that the maximum solar energy received inside the greenhouse for the N-S orientation was at 10:00 AM by the eastern roofs and at 13:00 to 14:00 by the western roofs. Thus, compared to the E-W orientation, there is better concordance between the time of receiving maximum radiation and heating needs of the greenhouse. At solar noon, the intensity of the total radiation and possible surplus energy were reduced.

## 4. CONCLUSIONS

This study managed to determine the optimum orientation of the greenhouses for Hemmatabad region located in the central part of Iran. For this purpose, a comparison was made between the irradiation received on the outer surface of the greenhouse cover and the irradiation captured inside the multi-span greenhouse with three different orientations (N-S, E-W and NE-SW). The main findings of this research are given below.

1. The greenhouse in the N-S orientation received greater irradiation on the outer surface of the cover in winter. However, the irradiation captured inside the greenhouse for the E-W orientation was more than that in other orientations, pointing to the significance of the solar incidence angle in the rate of radiation transmission through the cover and their penetration into the greenhouse.
2. The E-W orientation was the best selection for greenhouses in the study area because in the cold season, it captured an average of  $361.48 \text{ MJ day}^{-1}$  more energy than that in the N-S orientation and  $341.29 \text{ MJ day}^{-1}$  more energy than that in the NE-SW orientation. In addition, energy saving methods such as insulating some greenhouse surfaces and storing surplus solar energy can also be useful in this regard.

- The north wall could not receive the beam radiation for all the orientations investigated, and the total irradiation captured by this section was the diffuse radiation and the ground-reflected radiation.
- In the N-S orientation, compared to the E-W orientation, there was better concordance between the time of receiving maximum radiation and heating needs of the greenhouse.

The method used in the current study can be used to model and study different shapes of greenhouses at all latitudes and other seasons of the year.

## 5. ACKNOWLEDGEMENT

The financial support provided by Department of Agricultural Machinery Engineering, University of Tehran, Iran, is dully acknowledged.

## NOMENCLATURE

$A_i$	Area of walls and roofs ( $m^2$ )
$I$	Total radiation on a horizontal surface ( $Wm^{-2}$ )
$I_b$	Beam radiation ( $Wm^{-2}$ )
$I_d$	Diffuse radiation ( $Wm^{-2}$ )
$R_d$	View factor of tilted surface to the sky
$R_r$	View factor of tilted surface to the ground
$S_i(t)$	Total solar radiation on various walls and roofs ( $Wm^{-2}$ )
$S_t$	Total solar radiation falling on the greenhouse cover (W)

### Greek letters

$\beta$	Slope of the surface with horizontal ( $^\circ$ )
$\gamma$	Surface azimuth angle ( $^\circ$ )
$\delta$	Declination angle of the sun ( $^\circ$ )
$\theta_i$	Angle of incidence ( $^\circ$ )
$\theta_z$	Zenith angle ( $^\circ$ )
$\rho$	Reflectivity of the ground
$\tau$	Transmissivity of the greenhouse cover
$\omega$	Hour angle ( $^\circ$ )
$\Phi$	Latitude angle of a place ( $^\circ$ )

## REFERENCES

- Duro, J.A., Lauk, C., Kastner, T., Erb, K.-H. and Haberl, H., "Global inequalities in food consumption, cropland demand and land-use efficiency: A decomposition analysis", *Global Environmental Change*, Vol. 64, (2020), 102124. (<https://doi.org/10.1016/j.gloenvcha.2020.102124>).
- Iddio, E., Wang, L., Thomas, Y., McMorrow, G. and Denzer, A., "Energy efficient operation and modeling for greenhouses: A literature review", *Renewable & Sustainable Energy Reviews*, Vol. 117, (2020), 109480. (<https://doi.org/10.1016/j.rser.2019.109480>).
- Taki, M., Rohani, A. and Rahmati-Joneidabad, M., "Solar thermal simulation and applications in greenhouse", *Information Processing in Agriculture*, Vol. 5, (2018), 83-113. (<https://doi.org/10.1016/j.inpa.2017.10.003>).
- Anonymous, Annual agricultural statistics, Organization agriculture, (2019). (<https://yazd.maj.ir>), (Accessed: 7 May 2019).
- FAO, Iranian National Census of Agriculture, Food and Agriculture Organization, (2014). (<http://www.fao.org>), (Accessed: 24 July 2020).
- Mohammadi, B., Ranjbar, S.F. and Ajabshirchi, Y., "Application of dynamic model to predict some inside environment variables in a semi-solar greenhouse", *Information Processing in Agriculture*, Vol. 5, (2018), 279-288. (<https://doi.org/10.1016/j.inpa.2018.01.001>).
- Shamim Ahamed, M., Guo, H. and Tanino, K., "Energy saving techniques for reducing the heating cost of conventional greenhouses", *Biosystems Engineering*, Vol. 178, (2019), 9-33. (<https://doi.org/10.1016/j.biosystemseng.2018.10.017>).
- Pishgar-Komleh, S.H., Omid, M. and Heidari, M.D., "On the study of energy use and GHG (greenhouse gas) emissions in greenhouse cucumber production in Yazd province", *Energy*, Vol. 59, (2013), 63-71. (<https://doi.org/10.1016/j.energy.2013.07.037>).
- Vadiee, A. and Martin, V., "Energy management in horticultural applications through the closed greenhouse concept, state of the art", *Renewable & Sustainable Energy Reviews*, Vol. 16, (2012), 5087-5100. (<https://doi.org/10.1016/j.rser.2012.04.022>).
- Zarezade, M. and Mostafaeipour, A., "Identifying the effective factors implementing the solar dryers for Yazd province, Iran", *Renewable & Sustainable Energy Reviews*, Vol. 57, (2016), 765-775. (<https://doi.org/10.1016/j.rser.2015.12.060>).
- Tiwari, G.N., Din, M., Srivastava, N.S.L., Jain, D. and Sodha, M.S., "Evaluation of solar fraction (Fn) for the north wall of a controlled environment greenhouse: An experimental validation", *International Journal of Energy Research*, Vol. 26, (2002), 203-215. (<https://doi.org/10.1002/er.776>).
- Gupta, M.J. and Chandra, P., "Effect of greenhouse design parameters on conservation of energy for greenhouse environmental control", *Energy*, Vol. 27, (2002), 777-794. ([https://doi.org/10.1016/S0360-5442\(02\)00030-0](https://doi.org/10.1016/S0360-5442(02)00030-0)).
- Ghosal, M.K. and Tiwari, G.N., "Mathematical modeling for greenhouse heating by using thermal curtain and geothermal energy", *Solar Energy*, Vol. 76, (2004), 603-613. (<https://doi.org/10.1016/j.solener.2003.12.004>).
- Gupta, R. and Tiwari, G.N., "Modeling of energy distribution inside greenhouse using concept of solar fraction with and without reflecting surface on north wall", *Building and Environment*, Vol. 40, (2005), 63-71. (<https://doi.org/10.1016/j.buildenv.2004.03.014>).
- Gupta, R., Tiwari, G.N., Kumar, A. and Gupta, A., "Calculation of total solar fraction for different orientation of greenhouse using 3D-shadow analysis in Auto-CAD", *Energy and Building*, Vol. 47, (2012), 27-34. (<https://doi.org/10.1016/j.enbuild.2011.11.010>).
- Attar, I., Naili, N., Khalifa, N., Hazami, M. and Farhat, A., "Parametric and numerical study of a solar system for heating a greenhouse equipped with a buried exchanger", *Energy Conversion and Management*, Vol. 70, (2013), 163-173. (<https://doi.org/10.1016/j.enconman.2013.02.017>).
- Bouadila, S., Kooli, S., Skouri, S., Lazaar, M. and Farhat, A., "Improvement of the greenhouse climate using a solar air heater with latent storage energy", *Energy*, Vol. 64, (2014), 663-672. (<https://doi.org/10.1016/j.energy.2013.10.066>).
- Zhang, L., Xu, P., Mao, J., Tang, X., Li, Z. and Shi, J., "A low cost seasonal solar soil heat storage system for greenhouse heating: Design and pilot study", *Applied Energy*, Vol. 156, (2015), 213-222. (<https://doi.org/10.1016/j.apenergy.2015.07.036>).
- Ghasemi-Mobtaker, H., Ajabshirchi, Y., Ranjbar, S.F. and Matloobi, M., "Solar energy conservation in greenhouse: Thermal analysis and experimental validation", *Renewable Energy*, Vol. 96, (2016), 509-519. (<https://doi.org/10.1016/j.renene.2016.04.079>).
- Shamim Ahamed, M., Guo, H. and Tanino, K., "A quasi-steady state model for predicting the heating requirements of conventional greenhouses in cold regions", *Information Processing in Agriculture*, Vol. 5, (2018), 33-46. (<https://doi.org/10.1016/j.inpa.2017.12.003>).
- Yildirim, N. and Bilir, L., "Evaluation of a hybrid system for a nearly zero energy greenhouse", *Energy Conversion and Management*, Vol. 148, (2017), 1278-1290. (<https://doi.org/10.1016/j.enconman.2017.06.068>).
- Wei, B., Guo, S., Wang, J., Li, J., Wang, J., Zhang, J., Qian, C. and Sun, J., "Thermal performance of single span greenhouses with removable back walls", *Biosystems Engineering*, Vol. 141, (2016), 48-57. (<https://doi.org/10.1016/j.biosystemseng.2015.11.008>).
- Von Elsner, B., Briassoulis, D., Waaijenberg, D., Mistriotis, A., von Zabeltitz, C., Grattraud, J., Russo, G. and Suay-Cortes, R., "Review of structural and functional characteristics of greenhouses in European union countries: Part I, Design requirements", *Journal of Agricultural Engineering Research*, Vol. 75, (2000), 1-16. (<https://doi.org/10.1006/jaer.1999.0502>).
- Kendirli, B., "Structural analysis of greenhouses: A case study in Turkey", *Building and Environment*, Vol. 41, (2006), 864-871. (<https://doi.org/10.1016/j.buildenv.2005.04.013>).
- Sethi, V.P., "On the selection of shape and orientation of a greenhouse: Thermal modeling and experimental validation", *Solar Energy*, Vol. 83, (2009), 21-38. (<https://doi.org/10.1016/j.solener.2008.05.018>).
- Singh, R.D. and Tiwari, G.N., "Energy conservation in the greenhouse system: A steady state analysis", *Energy*, Vol. 35, (2010), 2367-2373. (<https://doi.org/10.1016/j.energy.2010.02.003>).

27. Çakır, U. and Şahin, E., "Using solar greenhouses in cold climates and evaluating optimum type according to sizing, position and location: A case study", *Computers and Electronics in Agriculture*, Vol. 117, (2015), 245-257. (<https://doi.org/10.1016/j.compag.2015.08.005>).
28. El-Maghlany, W.M., Teamah, M.A. and Tanaka, H., "Optimum design and orientation of the greenhouses for maximum capture of solar energy in North tropical region", *Energy Conversion and Management*, Vol. 105, (2015), 1096-1104. (<https://doi.org/10.1016/j.enconman.2015.08.066>).
29. Stanciu, C., Stanciu, D. and Dobrovicescu, A., "Effect of greenhouse orientation with respect to E-W axis on its required heating and cooling loads", *Energy Procedia*, Vol. 85, (2016), 498-504. (<https://doi.org/10.1016/j.egypro.2015.12.234>).
30. Chen, C., Li, Y., Li, N., Wei, S., Yang, F., Ling, H., Yu, N. and Han, F., "A computational model to determine the optimal orientation for solar greenhouses located at different latitudes in China", *Solar Energy*, Vol. 165, (2018), 19-26. (<https://doi.org/10.1016/j.solener.2018.02.022>).
31. Ghasemi-Mobtaker, H., Ajabshirchi, Y., Ranjbar, S.F. and Matloobi, M., "Simulation of thermal performance of solar greenhouse in north-west of Iran: An experimental validation", *Renewable Energy*, Vol. 135, (2019), 88-97. (<https://doi.org/10.1016/j.renene.2018.10.003>).
32. Chen, J., Ma, Y. and Pang, Z., "A mathematical model of global solar radiation to select the optimal shape and orientation of the greenhouses in southern China", *Solar Energy*, Vol. 205, (2020) 380-389. (<https://doi.org/10.1016/j.solener.2020.05.055>).
33. Baghestani Maybodi, N., Baghestani Maybodi, M.A. and Soufizadeh, S., "Pruning height and its effect on quantitative and qualitative seed production in old saxual (*Haloxylon aphyllum*) forests of Yazd, Iran", *Desert*, Vol. 11, (2006), 27-33. (<https://doi.org/10.22059/jdesert.2006.31864>).
34. Erbs, D.G., Klein, S.A. and Duffie, J.A., "Estimation of the diffuse radiation fraction for hourly, daily and monthly-average global radiation", *Solar Energy*, Vol. 28, (1982), 293-302. ([https://doi.org/10.1016/0038-092X\(82\)90302-4](https://doi.org/10.1016/0038-092X(82)90302-4)).
35. Duffie, J.A. and Beckman, W.A., *Solar engineering of thermal processes*, Fourth Ed., John Wiley & Son, New Jersey, (2013). (<https://doi.org/10.1002/9781118671603>).
36. Sethi, V.P. and Sharma, S.K., "Thermal modeling of a greenhouse integrated to an aquifer coupled cavity flow heat exchanger system", *Solar Energy*, Vol. 81, (2007), 723-741. (<https://doi.org/10.1016/j.solener.2006.10.00-2>).
37. Mertens, K., *Photovoltaics: Fundamentals, technology and practice*, First Ed., John Wiley & Sons, Chichester, UK, (2014). (<https://www.google.com/books/edition/Photovoltaics/AMNcDwAAQBAJ?hl=en&gbpv=1&dq=Mertens,+K.,+Photovoltaics+:+fundamentals,+technolog+y+and+practice+first+edition&pg=PR14&printsec=frontcover>).
38. Godbey, L.C., Bond, T. and Zornig, E.H.F., "Transmission of solar and long-wavelength energy by materials used as covers for solar collectors and greenhouses", *Transactions of the ASAE*, Vol. 22, (1979), 1137-1144. (<https://doi.org/10.13031/2013.35169>).
39. Kitani, O. and Jungbluth, T., *CIGR handbook of agricultural engineering*, ASAE Publications, St. Joseph, Michigan, (1999). (<https://doi.org/10.13031/2013.36337>).
40. Berroug, F., Lakhel, E.K., El Omari, M., Faraji, M. and El Qarnia, H., "Thermal performance of a greenhouse with a phase change material north wall", *Energy and Building*, Vol. 43, (2011), 3027-3035. (<https://doi.org/10.1016/j.enbuild.2011.07.020>).